

Photoinduced Weyl semimetal phase and anomalous Hall effect in a three-dimensional topological insulator

Meng-Nan Chen(陈梦南) and Wen-Chao Chen(陈文潮)

Citation: Chin. Phys. B, 2021, 30 (**11**): 110308. DOI: 10.1088/1674-1056/abff29
Journal homepage: http://cpb.iphy.ac.cn; http://iopscience.iop.org/cpb

What follows is a list of articles you may be interested in

Non-Hermitian quasicrystal in dimerized lattices

Longwen Zhou(周龙文) and Wenqian Han(韩雯岍)
Chin. Phys. B, 2021, 30 (**10**): 100308. DOI: 10.1088/1674-1056/ac1efc

High winding number of topological phase in non-unitary periodic quantum walk

Yali Jia(贾雅利) and Zhi-Jian Li(李志坚)
Chin. Phys. B, 2021, 30 (**10**): 100301. DOI: 10.1088/1674-1056/abf554

Review of quantum simulation based on Rydberg many-body system

Zheng-Yuan Zhang(张正源), Dong-Sheng Ding(丁冬生), and Bao-Sen Shi(史保森)
Chin. Phys. B, 2021, 30 (**2**): 020307. DOI: 10.1088/1674-1056/abd744

Metal-insulator phase transition and topology in a three-component system

Shujie Cheng(成书杰) and Xianlong Gao(高先龙)
Chin. Phys. B, 2021, 30 (**1**): 010302. DOI: 10.1088/1674-1056/abb305

Topological phase transitions driven by next-nearest-neighbor hopping in noncentrosymmetric cold Fermi gases

Wang Rui, Zhang Cun-Xi, Ji Qing-Shan
Chin. Phys. B, 2015, 24 (**3**): 030305. DOI: 10.1088/1674-1056/24/3/030305

RAPID COMMUNICATION

Photoinduced Weyl semimetal phase and anomalous Hall effect in a three-dimensional topological insulator*

Meng-Nan Chen(陈梦南)[1,†] and Wen-Chao Chen(陈文潮)[2,‡]

[1] School of Science, Hangzhou Dianzi University, Hangzhou 310018, China
[2] Institute of Advanced Magnetic Materials, College of Materials and Environmental Engineering, Hangzhou Dianzi University, Hangzhou 310018, China

(Received 10 March 2021; revised manuscript received 22 April 2021; accepted manuscript online 8 May 2021)

Motivated by the fact that Weyl fermions can emerge in a three-dimensional topological insulator on breaking either time-reversal or inversion symmetries, we propose that a topological quantum phase transition to a Weyl semimetal phase occurs under the off-resonant circularly polarized light, in a three-dimensional topological insulator, when the intensity of the incident light exceeds a critical value. The circularly polarized light effectively generates a Zeeman exchange field and a renormalized Dirac mass, which are highly controllable. The phase transition can be exactly characterized by the first Chern number. A tunable anomalous Hall conductivity emerges, which is fully determined by the location of the Weyl nodes in momentum space, even in the doping regime. Our predictions are experimentally realizable through pump-probe angle-resolved photoemission spectroscopy and raise a new way for realizing Weyl semimetals and quantum anomalous Hall effects.

Keywords: Floquet theory, Weyl semimetal, topological phase transition, Hall conductivity

PACS: 05.60.Gg, 03.65.Vf, 31.10.+z, 73.20.Mf **DOI:** 10.1088/1674-1056/abff29

1. Introduction

In recent years, topological phases in periodically driven quantum systems have attracted a great surge of research interest. Based on the Floquet theory, such engineering has led to various theoretical proposals and experiments to produce Floquet topological insulators, Floquet topological superconductors, and Floquet Weyl semimetals (WSMs) in many contexts, such as the solid-state, atomic, and photonic systems.[1–27] The topology in these systems is defined in terms of the Floquet states, i.e., the eigenstates of the single particle time evolution operator over one time period in the driven systems. The corresponding Floquet topological indices can therefore be defined in terms of the Floquet states, which are similar to their equilibrium analog.[3,28,29] The Floquet systems may also host unique topological phenomena without counterparts in static systems. For example, the discrete time crystal, which breaks continuous time translation symmetry and cannot exist in a static system.[30]

Much effort has been devoted to searching for Weyl fermions in three-dimensional (3D) materials both theoretically[31–36] and experimentally[37–41] recently because they exhibit a variety of interesting effects, including surface Fermi arc states and chiral magnetotransport. Weyl materials are usually manipulated by symmetry-breaking perturbations, such as the traditional application of strain, doping or static magnetic or electric fields. In contrast, Floquet engineering provides a more controllable way due to its high tunability. For noninteracting systems, the driving should be restricted to the off-resonant limit to prevent the system from being heated, with the frequency much larger than the energy scale of the system. Under this condition, the ground state for the system is still well-defined and an effective static Hamiltonian can be obtained, as clarified in the theoretical work of Kitagawa *et al.* for graphene and surface state of a 3D topological insulator,[42] where a topological phase transition from two-dimensional (2D) Dirac semimetal to quantum anomalous Hall (QAH) insulator was driven by light, which was in excellent agreement with later experiments.[4] This enables zero-temperature topological phases to exist in such nonequilibrium driving system. Therefore, we can use the standard quantum transport theory to deal with the spin and electron transport problems. The idea was soon extended to other 2D materials, including silicene and HgTe quantum well,[7,8] as well as 3D materials like Na_3Bi[9] and nodal-line semimetals,[10–15] where both type-I and type-II WSMs can be realized and other various topological phases with interesting transport phenomena can emerge. The Floquet WSM phase with multi-Weyl nodes was also proposed in crossing nodal-line semimetals.[1,16,18] However, for interacting systems, off-resonant driving just postpones runaway heating for exponentially long time, where topologi-

*Project supported by the National Natural Science Foundation of China (Grant No. 11804070) and Zhejiang Provincial Natural Science Foundation of China (Grant No. LQ19A040007).

†Corresponding author. E-mail: mnchen@hdu.edu.cn
‡Corresponding author. E-mail: cwc@hdu.edu.cn

© 2021 Chinese Physical Society and IOP Publishing Ltd

cal phases can not exist. Nandkishore *et al.*[43] pointed out that many-body localized systems can avoid energy absorption from off-resonant driving by a local Hamiltonian, which ensures the occurrence of spontaneous breaking of the time continuous translation symmetry and leads to the discovery of discrete time crystal.[30,44]

In this paper, we demonstrate that a 3D topological insulator can be driven into a WSM by applying an off-resonant circularly polarized light, which acts effectively as a tunable Zeeman exchange field and an additional Dirac mass term. The Floquet Weyl nodes appear as critical points in the momentum space separating a QAH phase of the effective 2D system from an ordinary insulator phase, where the Dirac mass gap closes. We also study the anomalous Hall conductivities, including a disorder-averaged part which contains the contribution of electrons at the Fermi surface and an intrinsic part contributed by electrons below the Fermi surface. In the DC limit, the intrinsic Hall conductivity remains quantized when the Fermi energy is sufficiently close to the Weyl nodes. This approach is highly controllable by the intensity of light and provides an alternative method to realize the WSMs and QAH effects.

This paper is organized as follow. In Section 2, we introduce the model construction. The first Chern numbers for the system are derived, which reveals the topological nature of the system and determines the locations of the Weyl nodes in momentum space. In Section 3, we discuss the anomalous Hall conductivities in δ-correlated impurity potential. We conclude in Section 4.

2. Model construction and the first Chern number

Let us begin by considering the low-energy $\boldsymbol{k}\cdot\boldsymbol{p}$ effective Hamiltonian

$$H=\varepsilon_{\boldsymbol{k}}\hat{\sigma}_0+\mathcal{A}_1 k_z\hat{\tau}_x\hat{\sigma}_z+\mathcal{A}_2\hat{\tau}_x(k_x\hat{\sigma}_x+k_y\hat{\sigma}_y)+M_{\boldsymbol{k}}\hat{\tau}_z, \quad (1)$$

which was used to describe the strong TI of Bi_2Se_3.[45] Here, $\hat{\sigma}_i$ and $\hat{\tau}_i$ ($i=0$, x, y, or z) denote the Pauli matrices in spin and orbital spaces, respectively, $M_{\boldsymbol{k}}=M_0-B_1k_z^2-B_2\boldsymbol{k}_\parallel^2$ with $\boldsymbol{k}_\parallel^2=k_x^2+k_y^2$ is the Dirac mass term expanded to the second order of the momentum, and $\varepsilon_{\boldsymbol{k}}=C+D_1k_z^2+D_2\boldsymbol{k}_\parallel^2$. For convenience, the momentum is set to be dimensionless, by properly choosing the units of parameters in the model, namely, C, D_1, D_2, M_0, $\mathcal{A}_1$, $\mathcal{A}_2$, B_1, and B_2. Making a unitary transformation $\mathcal{H}=U^\dagger HU$ with

$$U=\frac{1}{2}(1+\hat{\tau}_x)+\frac{1}{2}(1-\hat{\tau}_x)\hat{\sigma}_z, \quad (2)$$

we obtain

$$\mathcal{H}=\varepsilon_{\boldsymbol{k}}\hat{\sigma}_0+\mathcal{A}_2(k_x\hat{\sigma}_x+k_y\hat{\sigma}_y)+(M_{\boldsymbol{k}}\hat{\tau}_z+\mathcal{A}_1k_z\hat{\tau}_x)\hat{\sigma}_z. \quad (3)$$

We can find that the degrees $\hat{\tau}_i$ and $\hat{\sigma}_i$ have totally been separated.

In the presence of circularly polarized light incident in the z direction, the vector potential is given as

$$\boldsymbol{A}(t)=A_0\big(\eta\sin(\omega t),\cos(\omega t),0\big), \quad (4)$$

with $\boldsymbol{E}(t)=\partial\boldsymbol{A}(t)/\partial t$, where $\eta=+\ (-)$ denotes the right (left) circularly polarized light and A_0 is the intensity of the light. By the Peierls substitution, $\boldsymbol{k}\to\boldsymbol{k}+e\boldsymbol{A}(t)$, we obtain the full time-periodic Hamiltonian $\mathcal{H}^\eta(\boldsymbol{k},t)$.

In the Floquet picture, when the frequency of the light is sufficiently high, we can get a static effective Hamiltonian in the off-resonant approximation[42]

$$\mathcal{H}_{\rm eff}\simeq\mathcal{H}_0+\frac{[\mathcal{H}_{-1},\mathcal{H}_1]}{\omega}+\mathcal{O}\left(\frac{1}{\omega^2}\right), \quad (5)$$

where

$$\mathcal{H}_n=\frac{1}{T}\int_0^T \mathrm{d}t\,\mathrm{e}^{\mathrm{i}n\omega t}\mathcal{H}(t) \quad (6)$$

denotes the n-th Fourier component of the time-periodic Hamiltonian and $T=2\pi/\omega$ is the time period. Substituting the expression for the full model Hamiltonian $\mathcal{H}^\eta(\boldsymbol{k},t)$ into Eq. (5), we derive the effective static Hamiltonian as

$$\mathcal{H}^\eta_{\rm eff}(\boldsymbol{k})=\mathcal{H}_0(\boldsymbol{k})+h_0(\boldsymbol{k})+h_1^\eta(\boldsymbol{k})+h_z^\eta(\boldsymbol{k}), \quad (7)$$

where $h_0(\boldsymbol{k})=(\varepsilon_{\boldsymbol{k}}+D_2\tilde{A}_0^2)\hat{\sigma}_0$, $h_1^\eta(\boldsymbol{k})=\Gamma_{\rm F}^\eta\hat{\tau}_z(k_x\hat{\sigma}_x+k_y\hat{\sigma}_y)$, and $h_z^\eta(\boldsymbol{k})=\Gamma_z^\eta\hat{\sigma}_z-B_2\tilde{A}_0^2\hat{\tau}_z\hat{\sigma}_z$ with $\Gamma_z^\eta=\eta\tilde{A}_0^2\mathcal{A}_2^2/\omega$ acting as the effective Zeeman g-factor and the intensity of the light $\tilde{A}_0=eA_0$, and the Fermi velocity renormalized term $\Gamma_{\rm F}^\eta=2\eta B_2\mathcal{A}_2\tilde{A}_0^2/\omega$. We can find that $h_0(\boldsymbol{k})$ differs from $\varepsilon_{\boldsymbol{k}}$ only by a trivial shift in the Fermi energy. For the purpose of this work, we will set the $h_0(\boldsymbol{k})$ term to be zero as it does not affect the main physics. According to the band structures from *ab initio* calculations,[45] the parameters are taken to be $M_0=0.1$, $A_1=0.7$, $A_2=1.0$, $B_1=2.5$, $B_2=10$ and we typically take $\omega=20$ as a high frequency compared to the energy scale in our system. We also confine the light intensity $\tilde{A}_0$ around 0.1, which permits the $\Gamma_{\rm F}^\eta$ term to be neglected. In what follows, without loss of generality, we will focus on the $\eta=+$ case and drop the polarization label for notational simplicity. Now we can rewrite the full effective Hamiltonian as

$$\mathcal{H}_{\rm eff}=\mathcal{A}_2(k_x\hat{\sigma}_x+k_y\hat{\sigma}_y)+\big[M_{\boldsymbol{k}}^{\rm r}\hat{\tau}_z+\mathcal{A}_1k_z\hat{\tau}_x+\Gamma_z\big]\hat{\sigma}_z, \quad (8)$$

where $M_{\boldsymbol{k}}^{\rm r}=M_{\boldsymbol{k}}-B_2\tilde{A}_0^2$ denotes the renormalized Dirac mass.

The eigenstates of Hamiltonian (8) can be easily solved by first diagonalizing the operator in the square bracket. The eigenvalues are obtained as $\Delta_\kappa(\boldsymbol{k})=\Gamma_z+\kappa\lambda(\boldsymbol{k})$ with $\kappa=\pm$ and $\lambda(\boldsymbol{k})=\sqrt{(M_{\boldsymbol{k}}^{\rm r})^2+\mathcal{A}_1^2k_z^2}$. The corresponding eigenvectors are $\phi_+(\boldsymbol{k})=\big[\mathrm{sgn}(\mathcal{A}_1k_z)\cos\theta_{\boldsymbol{k}},\sin\theta_{\boldsymbol{k}}\big]^{\rm T}$ and $\phi_-(\boldsymbol{k})=\big[\mathrm{sgn}(\mathcal{A}_1k_z)\sin\theta_{\boldsymbol{k}},-\cos\theta_{\boldsymbol{k}}\big]^{\rm T}$, where $2\theta_{\boldsymbol{k}}=$

arccot$(M^{\rm r}_{\boldsymbol{k}}/|A_1 k_z|)$. Then the eigenvalues and eigenvectors for the Hamiltonian can be obtained as

$$E^{\rm v(c)}_{\kappa}(\boldsymbol{k}) = -(+)\sqrt{\mathcal{A}_2^2 k_\parallel^2 + \Delta^2_{\kappa}(\boldsymbol{k})}, \tag{9}$$

$$\psi^{\rm v(c)}_{\kappa}(\boldsymbol{k}) = \phi_{\kappa}(\boldsymbol{k}) \otimes \chi^{\rm v(c)}_{\kappa}(\boldsymbol{k}), \tag{10}$$

with superscript v (c) representing the valence (conduction) bands, where $\chi^{\rm v}_{\kappa}(\boldsymbol{k}) = (\mathrm{e}^{-\mathrm{i}\varphi_{\boldsymbol{k}_\parallel}}\sin\alpha_{\boldsymbol{k}\kappa}, -\cos\alpha_{\boldsymbol{k}\kappa})^{\rm T}$ and $\chi^{\rm c}_{\kappa}(\boldsymbol{k}) = (\mathrm{e}^{-\mathrm{i}\varphi_{\boldsymbol{k}_\parallel}}\cos\alpha_{\boldsymbol{k}\kappa}, \sin\alpha_{\boldsymbol{k}\kappa})^{\rm T}$ are eigenvectors for the valence and conductance bands, $\mathrm{e}^{\mathrm{i}\varphi_{\boldsymbol{k}_\parallel}} = (k_x + \mathrm{i}k_y)/|\boldsymbol{k}_\parallel|$ and $2\alpha_{\boldsymbol{k}\kappa} = \text{arccot}[\Delta_{\kappa}(\boldsymbol{k})/(\mathcal{A}_2|\boldsymbol{k}_\parallel|)]$. In Fig. 1, we plot the eigenvalues of the Hamiltonian in Eq. (7), where we can find that the band structure is just raised by $h_0(\boldsymbol{k})$ and exhibits linear dispersion along the z direction in momentum space when k_z is chosen to be not far away form the Weyl nodes.

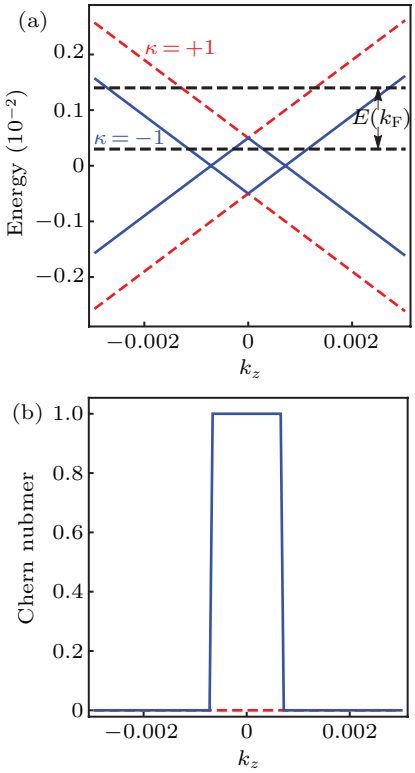


Fig. 1. (a) The band dispersion when $k_x = k_y = 0$ and (b) the first Chern numbers as functions of k_z, where two subbands for $\kappa = -$ touch at the Weyl nodes with nonzero first Chern number. The parameters are chosen to be $M_0 = 0.1$, $\mathcal{A}_1 = 0.7$, $\mathcal{A}_2 = 1.0$, $B_1 = 2.5$, $B_2 = 10$, $\tilde{A}_0 = 0.1$, and $\omega = 20$. Black dashed lines represent two different values for Fermi energies.

When the valance bands are fully filled and the conduction bands remain empty, there may exist an intrinsic quantum anomalous Hall conductivity, which is directly related to the first Chern number.[46] When k_z is treated as a parameter, the Hamiltonian in Eq. (8) is equivalent to a 2D system, for which the first Chern number can be defined as

$$C_{\kappa}(k_z) = \frac{1}{2\pi}\int \mathrm{d}k_x \mathrm{d}k_y F^{\rm v}_{\kappa}(\boldsymbol{k}_\parallel, k_z)\ , \tag{11}$$

where $F^{\rm v}_{\kappa}(\boldsymbol{k}_\parallel, k_z) = \mathrm{i}\hat{\boldsymbol{e}}_z \cdot [\nabla_\parallel \times \langle \psi^{\rm v}_{\kappa}(\boldsymbol{k})|\nabla_\parallel|\psi^{\rm v}_{\kappa}(\boldsymbol{k})\rangle]$ is the Berry curvature for the valance band and $\nabla_\parallel = (\partial_{k_x}, \partial_{k_y})$. It is convenient to put the integration in Eq. (11) into the cylinder coordinate system, where the gradient operator can be written as $\nabla_\parallel = \hat{\boldsymbol{e}}_{k_\parallel}\partial_{k_\parallel} + \hat{\boldsymbol{e}}_{\varphi_{\boldsymbol{k}_\parallel}}(1/k_\parallel)\partial_{\varphi_{\boldsymbol{k}_\parallel}}$. Noticing that $\partial_{k_\parallel}\hat{\boldsymbol{e}}_{\varphi_{\boldsymbol{k}_\parallel}} = 0$ and $\partial_{\varphi_{\boldsymbol{k}_\parallel}}\hat{\boldsymbol{e}}_{\varphi_{\boldsymbol{k}_\parallel}} = -\hat{\boldsymbol{e}}_{k_\parallel}$, a straightforward algebraic manipulation yields

$$F^{\rm v}_{\kappa}(\boldsymbol{k}_\parallel, k_z) = \frac{1}{2k_\parallel}\frac{\partial}{\partial k_\parallel}P^{\rm v}_{\kappa}(k_\parallel, k_z), \tag{12}$$

with

$$P^{\rm v}_{\kappa}(k_\parallel, k_z) = 2\mathrm{i}\langle\psi^{\rm v}_{\kappa}(\boldsymbol{k})|\partial_{\varphi_{\boldsymbol{k}_\parallel}}|\psi^{\rm v}_{\kappa}(\boldsymbol{k})\rangle. \tag{13}$$

Substituting Eqs. (12) and (13) into Eq. (11), we obtain the first Chern numbers as

$$\begin{aligned} C_{\kappa}(k_z) &= \frac{1}{2}[P^{\rm v}_{\kappa}(\infty, k_z) - P^{\rm v}_{\kappa}(0, k_z)] \\ &= \frac{1}{2}(1 - \cos 2\alpha_{\boldsymbol{k}\kappa})\Big|_0^{\infty} \\ &= \frac{1}{2}\big(\mathrm{sgn}[\Delta_{\kappa}(k_\parallel = 0, k_z)] - \mathrm{sgn}[\kappa]\big). \end{aligned} \tag{14}$$

The Chern numbers are functions of k_z for a given light intensity $\tilde{A}_0$, as shown in Fig. 2(b). The corresponding non-trivial Berry phase structure is shown in Fig. 2(b). In Fig. 2(a), we plot the phase diagram for both k_z and $\tilde{A}_0$. The first Chern numbers are directly related to the quantized Hall conductivities by[46]

$$\sigma_{xy} = \frac{e^2}{h}C_{\kappa}(k_z). \tag{15}$$

One can easily find from Eqs. (10) and (14) that there exist two critical points $(0, 0, \pm k^{\rm c}_{\rm w})$ where the energy bands touch and the first Chern numbers change, which precisely depicts the topological phase transition. It suggests the existence of open surface states connecting the two critical points, which are known as the Fermi arcs. The value of $k^{\rm c}_{\rm w}$ can be solved from the relation $E^{\rm v(c)}_{-}(\boldsymbol{k}) = 0$. These two critical points are known as the Weyl nodes. Then the total anomalous Hall conductivities can be obtained as

$$\sigma_{\rm aH} = \int_{\rm BZ}\frac{\mathrm{d}k_z}{2\pi}\sigma_{xy} = \frac{k^{\rm c}_{\rm w}}{\pi}\frac{e^2}{h}. \tag{16}$$

In Section 3, we will derive Eq. (16) in more detail in terms of the Kubo formula. We rewrite Hamiltonian (8) in a diagonal form by applying a unitary transformation in $\hat{\tau}$-space as

$$\mathcal{H}_{\rm eff} = \begin{pmatrix} h_+(\boldsymbol{k}) & 0 \\ 0 & h_-(\boldsymbol{k}) \end{pmatrix}, \tag{17}$$

and it should be noted that only subbands for $\kappa = -1$ support the Weyl nodes. Then we expand the $h_-(\boldsymbol{k})$ to linear order of $\boldsymbol{k}$ around the Weyl nodes, followed by applying a rotation in the $\boldsymbol{k}_\parallel$ plane and making some rescaling. This yields the standard Weyl Hamiltonian

$$h^{\chi}_{\rm Weyl}(\boldsymbol{k}) = \chi v_{\rm F}\sum_{i=x,y,z} k_i\hat{\sigma}_i, \tag{18}$$

where $\chi = \pm$ denotes the chirality of the two Weyl nodes and $v_{\rm F}$ is the Fermi velocity, whose value is very close to $\mathcal{A}_2$ since the band dispersion is linearized near the Weyl nodes, which is clearly illustrated in Fig. 1. So in what follows, we will use $v_{\rm F}$ to replace $\mathcal{A}_2$ for convenience.

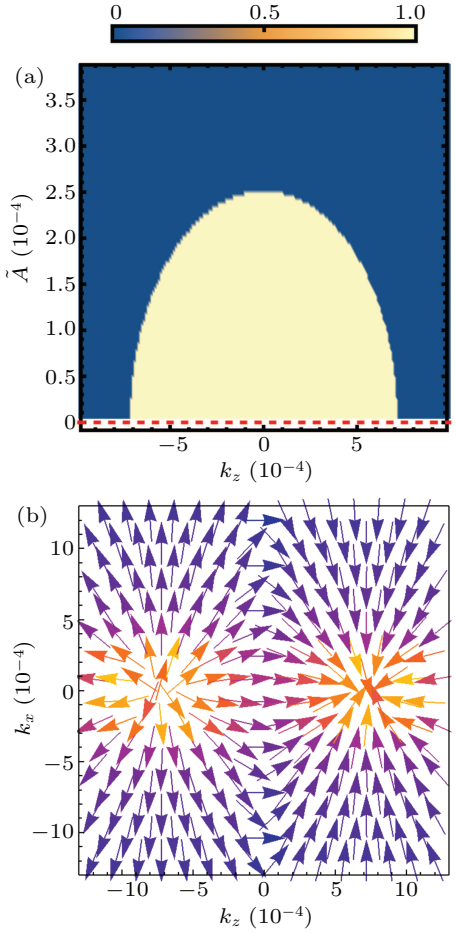


Fig. 2. (a) Topological phase diagram determined from the first Chern numbers in the k_z–$\tilde{A}$ plane, where $\tilde{A} = \tilde{A}_0 - 0.1$ is the artificially shifted light intensity. The other parameters are the same as those in Fig. 1. The red dashed line is used to label the value of $\tilde{A}$ for which the distance between Weyl nodes in momentum space is the largest. (b) Field lines of the Berry curvature in the $k_y = 0$ plane.

3. The disorder averaged anomalous Hall conductivity

The discussions in the last section tell us that the main effect of an off-resonant circular polarized light is the generation of a time-reversal symmetry breaking perturbation. Therefore, the WSM phase and the anomalous Hall effect emerge naturally. In this section, we will explore the impurity-averaged anomalous Hall conductivity in the periodically driving system.

3.1. Impurity-averaged Hall conductivity at the Fermi surface

We consider the white-noise spin-independent random potential with zero mean value $\langle V(\boldsymbol{r})\rangle_{\rm imp} = 0$ and correlation function

$$\zeta(\boldsymbol{r}-\boldsymbol{r}') = \langle V(\boldsymbol{r})V(\boldsymbol{r}')\rangle_{\rm imp} = n_{\rm i}V_0^2\delta(\boldsymbol{r}-\boldsymbol{r}'), \tag{19}$$

whose form in the momentum space is given by

$$\zeta_{\boldsymbol{k}} = \int \zeta(\boldsymbol{r})\mathrm{e}^{-\mathrm{i}\boldsymbol{k}\cdot\boldsymbol{r}}\,\mathrm{d}\boldsymbol{r} = n_{\rm i}V_0^2, \tag{20}$$

with $n_{\rm i}$ the density of impurities.

The averaging over disorder turns the infinitesimal increment $\mathrm{i}0^+ \to \mathrm{i}/2\tau$ of the retarded Green's function into a finite constant, which defines the inverse of the elastic scattering time. Therefore, the disorder averaged retarded (advanced) Green's function can be written as a general form

$$G^{\rm R(A)}_{\mu\kappa}(\boldsymbol{k}) = \frac{\hat{P}^{\mu}_{\kappa}(\boldsymbol{k})}{\varepsilon - E^{\mu}_{\kappa}(\boldsymbol{k}) + (-)\mathrm{i}/2\tau_{\kappa}}, \tag{21}$$

where $\hat{P}^{\mu}_{\kappa}(\boldsymbol{k}) = |\psi^{\mu}_{\kappa}(\boldsymbol{k})\rangle\langle\psi^{\mu}_{\kappa}(\boldsymbol{k})|$ denotes the project operator with $\mu = \mathrm{v},\mathrm{c}$ the band indices. In what follows we will assume, for concreteness, that the Fermi level lies in the conduction band. In the self-consistent Born approximation, the perturbed Green's function can be calculated as

$$\begin{aligned} G_{\mu\kappa}(\boldsymbol{k}) &= G^0_{\mu\kappa}(\boldsymbol{k}) \\ &\quad + G^0_{\mu\kappa}(\boldsymbol{k})\int \frac{\mathrm{d}^3\boldsymbol{k}'}{(2\pi)^2}\zeta_{\boldsymbol{k}'}G_{\mu\kappa}(\boldsymbol{k}')G_{\mu\kappa}(\boldsymbol{k}), \end{aligned} \tag{22}$$

where $G^0_{\mu\kappa}(\boldsymbol{k})$ is the unperturbed Green's function. The retarded impurity self-energy can be given as

$$\Sigma^{\rm R}_{\kappa}(\boldsymbol{k}) = n_{\rm i}V_0^2\int \frac{\mathrm{d}^3\boldsymbol{k}'}{(2\pi)^3}\frac{|\langle\psi^{\rm c}_{\kappa}(\boldsymbol{k})|\psi^{\rm c}_{\kappa}(\boldsymbol{k}')\rangle|^2}{\varepsilon - E^{\rm c}_{\kappa}(\boldsymbol{k}') + \mathrm{i}/2\tau_{\kappa}}, \tag{23}$$

where we have adopted the weak scattering condition, under which the valence band contribution can be neglected. The imaginary part of the self-energy can be derived to be

$$\begin{aligned} \left|\mathrm{Im}\Sigma^{\rm R}_{\kappa}(\boldsymbol{k})\right| &= \frac{1}{2\tau_{\kappa}} \\ &= \frac{1}{2\tau_{\kappa 0}}\left(1 + \frac{\Delta_{\kappa}(\boldsymbol{k})\langle\Delta_{\kappa}(\boldsymbol{k})\rangle}{E_{\rm F}^2}\right), \end{aligned} \tag{24}$$

where $1/\tau_{\kappa 0} = \pi n_{\rm i}V_0^2 g_{\kappa}(E_{\rm F})$ with the density of states

$$g_{\kappa}(E_{\rm F}) = \int \frac{\mathrm{d}^3\boldsymbol{k}}{(2\pi)^3}\delta\left(E^{\rm c}_{\kappa}(\boldsymbol{k}) - E_{\rm F}\right), \tag{25}$$

and

$$\langle\Delta_{\kappa}(\boldsymbol{k})\rangle = \frac{1}{g_{\kappa}(E_{\rm F})}\int \frac{\mathrm{d}^3\boldsymbol{k}}{(2\pi)^3}\Delta_{\kappa}(\boldsymbol{k})\delta\left(E^{\rm c}_{\kappa}(\boldsymbol{k}) - E_{\rm F}\right). \tag{26}$$

In the analysis below, we will neglect the $\boldsymbol{k}_{\parallel}^2$ correction to the linear Hamiltonian, as the main contribution to the minimal conductivity comes from the vicinity of the $\boldsymbol{k}_{\parallel} = 0$ point, when the Fermi surface is sufficiently close to the Weyl nodes. Under this condition, $\tau_{\kappa}\tau^{-1}_{\kappa 0}$ can be solved from Eq. (24) approximately by expanding to linear order of $\Delta_{\kappa}/E_{\rm F}$ as

$$\tau_{\kappa}\tau^{-1}_{\kappa 0} \simeq 1 - \frac{\Delta_{\kappa}\langle\Delta_{\kappa}\rangle}{E_{\rm F}^2}, \tag{27}$$

which will be useful in the following discussion. Noticing that the photon dressed term originating from $\boldsymbol{k}_\parallel^2$ terms should be kept, as it affects largely in our system. The integral in Eq. (25) can be performed in the cylindrical coordinate by transforming the measure $\int \mathrm{d}k_z \mathrm{d}k_x \mathrm{d}k_y \to \int \mathrm{d}k_z \int \mathrm{d}\theta k_\parallel \mathrm{d}k_\parallel$, yielding

$$g_\kappa(E_\mathrm{F}) = \frac{E_\mathrm{F}}{4\pi^2 v_\mathrm{F}^2} \int_{\mathrm{BZ}} \mathrm{d}k_z \Theta\big(E_\mathrm{F} - |\Delta_\kappa(k_z)|\big), \tag{28}$$

where the integral over k_z is constrained in the first Brillouin zone and Θ is the Heaviside step function.

In the following, we adopt the method developed by Burkov.[47] We start by introducing the current–current correlation function in the standard Kubo formula, which has the form[49]

$$\Pi_{\alpha\beta}(q) = \frac{1}{V\beta} \sum_k \mathrm{Tr}\big[J_{\boldsymbol{k}\alpha} G(k+q) \tilde{J}_{\boldsymbol{k}\beta} G(k)\big], \tag{29}$$

where $k = (\mathrm{i}\omega_m, \boldsymbol{k})$, $q = (\mathrm{i}\Omega_n, \boldsymbol{q})$ denote the four-component momentum with ω_m and Ω_n denoting fermionic and bosonic Matsubara frequencies, respectively. $J_{\boldsymbol{k}\alpha} = (J_{\boldsymbol{k}0}, J_{\boldsymbol{k}i})$ is the four-component U(1) conservation current, in which $J_{\boldsymbol{k}0} = e\hat{\sigma}_0$ is the charge component, $J_{\boldsymbol{k}i} = \frac{e\partial \mathcal{H}_\mathrm{eff}}{\hbar \partial k_i}$ with $i = x,y,z$ is the unperturbed spatial current, which can be written approximately as $J_{\boldsymbol{k}i} \simeq e v_\mathrm{F} \hat{\sigma}_i$ when we are interested in the states around the Fermi surface. Specifically, $\tilde{J}_{\boldsymbol{k}i}$ is the impurity-dressed spatial current, which will be obtained by calculating the dressed vertex shown by the Feynman diagram in Fig. 3(a). Here, we only consider the ladder diagram summation, which is known as the diffusion propagator, as Fig. 3(b) shows. The diffusion propagator can be defined as

$$D(k^0, k^0+q) = \frac{1}{\hat{1} - \Xi(k^0, k^0+q)}, \tag{30}$$

where $\hat{1}$ denotes the identity matrix and

$$\begin{aligned} &\Xi_{\alpha\beta}(k^0, k^0+q) \\ &= \frac{n_\mathrm{i} V_0^2}{2} \int \frac{\mathrm{d}^3\boldsymbol{k}}{(2\pi)^3} \mathrm{Tr}\big[\hat{\sigma}_\alpha G(k+q) \hat{\sigma}_\beta G(k)\big] \end{aligned} \tag{31}$$

is the ladder insertion. Note that Eq. (31) is the charge–spin or spin–spin correlation function, based on the choice of indices α and β. After doing the analytic continuation $\mathrm{i}\Omega_n \to \Omega + \mathrm{i}\eta$ and $\mathrm{i}\omega_m \to \varepsilon \pm \mathrm{i}\eta$, the Green's functions and the ladder insertion are turned to be the retarded (R) and advanced (A) forms and the correlation function (29) thus can be divided into two parts:

$$\Pi_{\alpha\beta}(q) = \Pi^\mathrm{I}_{\alpha\beta}(q) + \Pi^\mathrm{II}_{\alpha\beta}(q), \tag{32}$$

where $\Pi^\mathrm{I}_{\alpha\beta}(q)$ is the the response contributed by states at the Fermi surface, which has the form

$$\begin{aligned} \Pi^\mathrm{I}_{\alpha\beta}(q) = \lambda^\mathrm{I} \int \frac{\mathrm{d}\varepsilon}{2\pi\mathrm{i}} \frac{\mathrm{d}n_\mathrm{F}(\varepsilon)}{\mathrm{d}\varepsilon} \\ \times \sum_\gamma \Xi^\mathrm{RA}_{\alpha\gamma}(k^0, k^0+q) D^\mathrm{RA}_{\gamma\beta}(k^0, k^0+q), \end{aligned} \tag{33}$$

$\gamma = 0,x,y,z$ and $\Pi^\mathrm{II}_{\alpha\beta}(q)$ is the response contributed by all states below the Fermi energy, which can be given by

$$\Pi^\mathrm{II}_{\alpha\beta}(q) = \lambda^\mathrm{II} \int \frac{\mathrm{d}\varepsilon}{2\pi\mathrm{i}} n_\mathrm{F}(\varepsilon) \mathrm{Im}\Xi^\mathrm{RR}_{\alpha\beta}(k^0, k^0+q). \tag{34}$$

We will make use of Eqs. (33) and (34), particularly the $0x$ component, to compute the Hall conductivity. The coefficients λ^I and λ^I are therefore given as $\lambda^\mathrm{I} = \frac{-2\Omega e^2 \nu_\mathrm{F}}{n_\mathrm{i} V_0^2}$ and $\lambda^\mathrm{II} = \frac{4\mathrm{i} e^2 \nu_\mathrm{F}}{n_\mathrm{i} V_0^2}$.

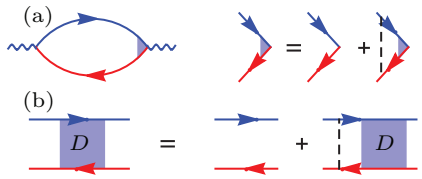


Fig. 3. (a) Feynman diagrams for the impurity averaged response function with the dressed vertex, in the presence of disorder (dashed lines). (b) The diffusion propagator with the ladder insertion.

Let us now find the explicit expression for $\Pi^\mathrm{I}_{0x}(q)$. Without loss of generality, $\boldsymbol{q}$ is taken as $\boldsymbol{q} = |\boldsymbol{q}|\hat{e}_y$, due to the presence of full rotational symmetry in xy plane. We can rewrite Eq. (33) as

$$\Pi^\mathrm{I}_{0x}(q) = \sum_{\kappa,\gamma} \Lambda_\kappa \Xi^\mathrm{RA}_{0\gamma}(k^0, k^0+q) D^\mathrm{RA}_{\gamma x}(k^0, k^0+q), \tag{35}$$

where $\Lambda_\kappa = \mathrm{i} e^2 \nu_\mathrm{F} \Omega \tau_{\kappa 0} g_\kappa(E_\mathrm{F})$. The calculations for matrix elements $\Xi^\mathrm{RA}_{\alpha\beta}(k^0, k^0+q)$ are straightforward by doing the gradient expansion to linear order of $|\boldsymbol{q}|$ when $|\boldsymbol{q}| \to 0$. By some algebra, those matrix elements are derived to be

$$\begin{aligned} \Xi^\mathrm{RA}_{00} &= \left\langle \frac{\tau_\kappa \tau^{-1}_{\kappa 0}}{1 - \mathrm{i}\Omega\tau_\kappa} \right\rangle, \quad \Xi^\mathrm{RA}_{xy} = \Xi^\mathrm{RA}_{yx} = 0, \\ \Xi^\mathrm{RA}_{0x} &= -\Xi^\mathrm{RA}_{x0} = \frac{\mathrm{i}|\boldsymbol{q}|v_\mathrm{F}}{2E_\mathrm{F}} \left\langle \frac{\Delta_\kappa}{E_\mathrm{F}} \frac{\tau_\kappa \tau^{-1}_{\kappa 0}}{1 - \mathrm{i}\Omega\tau_\kappa} \right\rangle, \\ \Xi^\mathrm{RA}_{0z} &= \Xi^\mathrm{RA}_{z0} = \left\langle \frac{\Delta_\kappa}{E_\mathrm{F}} \frac{\tau_\kappa \tau^{-1}_{\kappa 0}}{1 - \mathrm{i}\Omega\tau_\kappa} \right\rangle, \\ \Xi^\mathrm{RA}_{xz} &= -\Xi^\mathrm{RA}_{zx} = \frac{\mathrm{i}|\boldsymbol{q}|v_\mathrm{F}}{2E_\mathrm{F}} \left\langle \frac{\tau_\kappa \tau^{-1}_{\kappa 0}}{1 - \mathrm{i}\Omega\tau_\kappa} \right\rangle, \\ \Xi^\mathrm{RA}_{xx} &= \Xi^\mathrm{RA}_{yy} = \left\langle \frac{E_\mathrm{F}^2 - \Delta_\kappa^2}{2E_\mathrm{F}^2} \frac{\tau_\kappa \tau^{-1}_{\kappa 0}}{1 - \mathrm{i}\Omega\tau_\kappa} \right\rangle, \\ \Xi^\mathrm{RA}_{zz} &= \left\langle \frac{\Delta_\kappa^2}{E_\mathrm{F}^2} \frac{\tau_\kappa \tau^{-1}_{\kappa 0}}{1 - \mathrm{i}\Omega\tau_\kappa} \right\rangle. \end{aligned} \tag{36}$$

The definition of average $\langle \cdots \rangle$ here is the same as Eq. (26). Equation (35) then reads

$$\Pi^\mathrm{I}_{0x}(q) = \sum_\kappa \Lambda_\kappa \frac{\Xi^\mathrm{RA}_{0z} \Xi^\mathrm{RA}_{zx} + \Xi^\mathrm{RA}_{x0}(1 - \Xi^\mathrm{RA}_{zz})}{\Gamma(q)(1 - \Xi^\mathrm{RA}_{xx})}, \tag{37}$$

where

$$\Gamma(q) = \big(1 - \Xi^\mathrm{RA}_{00}\big)\big(1 - \Xi^\mathrm{RA}_{zz}\big) - \Xi^\mathrm{RA}_{0z} \Xi^\mathrm{RA}_{z0}, \tag{38}$$

which represents the $0z$-block of the diffusion propagator. Equation (27) allows us to approximate Eq. (38) as $\Gamma(0)=0$, which is known as the diffusion pole and agrees with the charge conservation Ward identity.[47,48] Combining Eqs. (36) and (37) and expanding $\Gamma(\Omega,0)$ to linear order of Ω, we obtain the full expression for $\Pi^{\mathrm{I}}_{0x}(q)$ as

$$\Pi^{\mathrm{I}}_{0x}(q) = \frac{-\mathrm{i}|\boldsymbol{q}|v_{\mathrm{F}}}{2E_{\mathrm{F}}}\sum_{\kappa}\Lambda_{\kappa}\left\langle\frac{\Delta_{\kappa}}{E_{\mathrm{F}}}\frac{\tau_{\kappa}\tau^{-1}_{\kappa 0}}{1-\mathrm{i}\Omega\tau_{\kappa}}\right\rangle \times\frac{1+\left\langle\frac{E_{\mathrm{F}}^2-\Delta_{\kappa}^2}{E_{\mathrm{F}}^2}\frac{\tau_{\kappa}\tau^{-1}_{\kappa 0}}{1-\mathrm{i}\Omega\tau_{\kappa}}\right\rangle}{1-\left\langle\frac{E_{\mathrm{F}}^2-\Delta_{\kappa}^2}{2E_{\mathrm{F}}^2}\frac{\tau_{\kappa}\tau^{-1}_{\kappa 0}}{1-\mathrm{i}\Omega\tau_{\kappa}}\right\rangle}\left[\frac{\partial\Gamma(\Omega,0)}{\partial(\Omega\tau_{\kappa 0})}\Omega\tau_{\kappa 0}\right]^{-1}. \tag{39}$$

In the limit $\Omega\to 0$ with fixed $\tau_{\kappa 0}$ (i.e., the diffusive limit), the above equation yields

$$\Pi^{\mathrm{I}}_{0x}(0,\boldsymbol{q}) = \frac{-\mathrm{i}|\boldsymbol{q}|e^2v_{\mathrm{F}}^2}{2E_{\mathrm{F}}}\sum_{\kappa}g_{\kappa}(E_{\mathrm{F}})\left\langle\frac{\Delta_{\kappa}}{E_{\mathrm{F}}}\tau_{\kappa}\tau^{-1}_{\kappa 0}\right\rangle K(\Delta_{\kappa}), \tag{40}$$

where

$$K(\Delta_{\kappa}) = \frac{1+\left\langle\frac{E_{\mathrm{F}}^2-\Delta_{\kappa}^2}{E_{\mathrm{F}}^2}\tau_{\kappa}\tau^{-1}_{\kappa 0}\right\rangle}{1-\left\langle\frac{E_{\mathrm{F}}^2-\Delta_{\kappa}^2}{2E_{\mathrm{F}}^2}\tau_{\kappa}\tau^{-1}_{\kappa 0}\right\rangle}\left[\frac{\partial\Gamma(\Omega,0)}{\partial(\Omega\tau_{\kappa 0})}\bigg|_{\Omega=0}\right]^{-1}. \tag{41}$$

The Hall conductivity at the Fermi surface therefore reads

$$\sigma^{\mathrm{I}}_{\mathrm{aH}} = \lim_{q\to 0}\frac{\Pi^{\mathrm{I}}_{0x}(q)}{|\boldsymbol{q}|} = \frac{-\mathrm{i}e^2v_{\mathrm{F}}^2}{2E_{\mathrm{F}}}\sum_{\kappa}g_{\kappa}(E_{\mathrm{F}})\left\langle\frac{\Delta_{\kappa}}{E_{\mathrm{F}}}\tau_{\kappa}\tau^{-1}_{\kappa 0}\right\rangle K(\Delta_{\kappa}). \tag{42}$$

Notice that $K(\Delta_{\kappa})=K(-\Delta_{\kappa})$. As a consequence, $\sigma^{\mathrm{I}}_{\mathrm{aH}}$ is an odd functional of Δ_{κ}. We compute Eq. (42) numerically with the variation of the Fermi energy, and the results are shown in Fig. 4(a). The values of the Fermi energy in two ranges are considered here, i.e., (i) $0<E_{\mathrm{F}}<\Delta_{-}(0)$ and (ii) $E_{\mathrm{F}}>\Delta_{-}(0)$, for which the Fermi energy crosses through $\kappa=-1$ subband while stays away from the conduction band for the $\kappa=+1$ sector and the Fermi level crosses through both $\kappa=-1$ and $\kappa=+1$ subbands, respectively, as Fig. 1(a) shows. We can find that for the case (i), $\sigma^{\mathrm{I}}_{\mathrm{aH}}=0$. This is because the Dirac mass $\Delta_{-}(k_z)$ changes sign at the Weyl nodes, i.e., $\Delta_{-}(k_z)$ is an odd function of $k_z-k_{\mathrm{w}}^{\mathrm{c}}$ and $k_z+k_{\mathrm{w}}^{\mathrm{c}}$, we can see that this property leads to a vanishing integral of k_z over the Fermi surface in Eq. (42). As we will see below, this phase is robust against the disorder and is usually referred as the Weyl metal phase.[47] When the Fermi energy is raised to be in the range $E_{\mathrm{F}}>\Delta_{-}(0)$, the impurity-averaged Hall conductivities for both sectors become nonzero, which leads to a nonzero value of $\sigma^{\mathrm{I}}_{\mathrm{aH}}$ and indicates that the system is in a anomalous Hall phase.

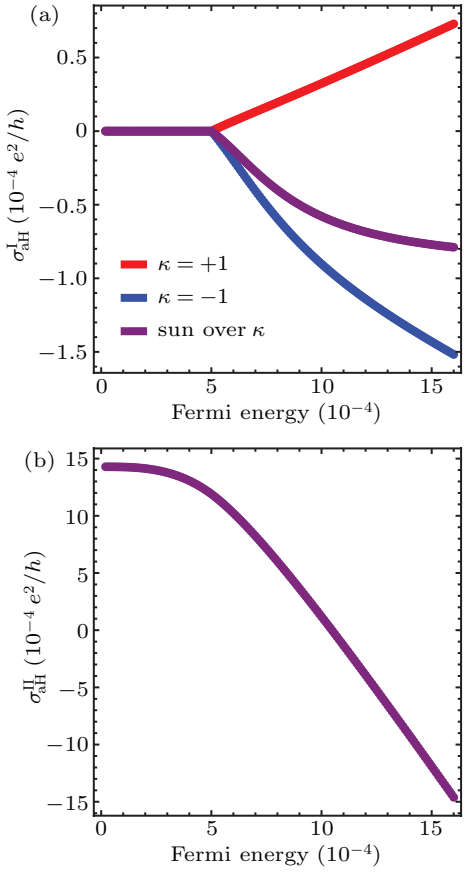


Fig. 4. (a) The impurity-averaged Hall conductivity and (b) the intrinsic Hall conductivity as a function of the Fermi energy, where we set $\tau_{\kappa 0}=1$.

3.2. Intrinsic Hall conductivity below the Fermi surface

In our analysis above, the focus has been on the contribution from electron states at the Fermi surface, whose behaviors are independent of the topological nature of the states. Now we would like to turn to the discussion of the contribution from electron states below the Fermi surface, i.e., the $0x$-component for $\Pi^{\mathrm{II}}_{\alpha\beta}(q)$, in contrast to $\Pi^{\mathrm{I}}_{\alpha\beta}(q)$, the $\Pi^{\mathrm{II}}_{\alpha\beta}(q)$ is directly related to the topological nature of the states. Equation (34) can be rewritten as

$$\Pi^{\mathrm{II}}_{0x}(q) = 2\mathrm{i}\int\frac{\mathrm{d}\varepsilon}{2\pi\mathrm{i}}n_{\mathrm{F}}(\varepsilon)\int\frac{\mathrm{d}^3\boldsymbol{k}}{(2\pi)^3} \times\mathrm{Im}\mathrm{Tr}\left[J_{\boldsymbol{k}0}G^{\mathrm{R}}(k+q)J_{\boldsymbol{k}x}G^{\mathrm{R}}(k)\right]. \tag{43}$$

Here, we should use the exact definition of the spatial component current operator as $J_{\boldsymbol{k}i}=\frac{e\partial\mathcal{H}_{\mathrm{eff}}}{\hbar\partial k_i}$, because the linearized and gapless band structure is not sufficient to characterize the properties of those electron states, for example, the topological properties. Substituting Eq. (21) into Eq. (43) and using the condition $1/\tau_{\kappa}\ll E_{\mathrm{F}}$ (the weak scattering condition), the evaluation for response contributed by all states below the Fermi energy can be performed as

$$\Pi^{\rm II}_{0x}(q)=\frac{e^2}{\hbar}\int\frac{{\rm d}^3\boldsymbol{k}}{(2\pi)^3}\sum_{\kappa}\sum_{\mu\nu}\left[\langle\psi^{\mu}_{\kappa}(\boldsymbol{k})|\psi^{\nu}_{\kappa}(\boldsymbol{k}+\boldsymbol{q})\rangle\left\langle\psi^{\nu}_{\kappa}(\boldsymbol{k}+\boldsymbol{q})\left|\frac{\partial\mathcal{H}_{\rm eff}}{\partial k_x}\right|\psi^{\mu}_{\kappa}(\boldsymbol{k})\right\rangle\right]\frac{n_{\rm F}(E^{\nu}_{\kappa}(\boldsymbol{k})-\hbar\Omega)-n_{\rm F}(E^{\mu}_{\kappa}(\boldsymbol{k}))}{\Omega-E^{\nu}_{\kappa}(\boldsymbol{k})+E^{\mu}_{\kappa}(\boldsymbol{k})}. \tag{44}$$

We can find that $\Pi^{\rm II}_{0x}(q)$ is insensitive to the impurity potential, hence it is robust against the disorder. This relation can be used to find the topological nature of the intrinsic Hall conductivity. In the limit of small q, the state vector $|\psi^{\nu}_{\kappa}(\boldsymbol{k}+\boldsymbol{q})\rangle$ can be expanded to linear order of $\boldsymbol{q}$, yielding

$$\begin{aligned}\langle\psi^{\mu}_{\kappa}(\boldsymbol{k})|\psi^{\nu}_{\kappa}(\boldsymbol{k}+\boldsymbol{q})\rangle &\simeq \delta_{\mu\nu}+\boldsymbol{q}\cdot\langle\psi^{\mu}_{\kappa}(\boldsymbol{k})|\partial_{\boldsymbol{k}}|\psi^{\nu}_{\kappa}(\boldsymbol{k})\rangle\\ &=\delta_{\mu\nu}+|\boldsymbol{q}|\langle\psi^{\mu}_{\kappa}(\boldsymbol{k})|\partial_{k_y}|\psi^{\nu}_{\kappa}(\boldsymbol{k})\rangle.\end{aligned} \tag{45}$$

Using the relation

$$\langle\psi^{\mu}_{\kappa}(\boldsymbol{k})|\partial_{k_\alpha}|\psi^{\nu}_{\kappa}(\boldsymbol{k})\rangle=\frac{\langle\psi^{\mu}_{\kappa}(\boldsymbol{k})|\frac{\partial\mathcal{H}_{\rm eff}}{\partial k_\alpha}|\psi^{\nu}_{\kappa}(\boldsymbol{k})\rangle}{-E^{\mu}_{\kappa}(\boldsymbol{k})+E^{\nu}_{\kappa}(\boldsymbol{k})}, \tag{46}$$

and noting that $\mu\neq\nu$, Eq. (44) can be written as

$$\begin{aligned}\Pi^{\rm II}_{0x}(q) &= \frac{e^2|\boldsymbol{q}|}{\hbar}\int\frac{{\rm d}^3\boldsymbol{k}}{(2\pi)^3}\sum_{\kappa,\mu\neq\nu}\mathcal{B}^{\mu\nu}_{xy}\left[-E^{\mu}_{\kappa}(\boldsymbol{k})+E^{\nu}_{\kappa}(\boldsymbol{k})\right]\\ &\times\frac{n_{\rm F}(E^{\mu}_{\kappa}(\boldsymbol{k})-\hbar\Omega)-n_{\rm F}(E^{\nu}_{\kappa}(\boldsymbol{k}))}{\Omega-E^{\mu}_{\kappa}(\boldsymbol{k})+E^{\nu}_{\kappa}(\boldsymbol{k})},\end{aligned} \tag{47}$$

where

$$\mathcal{B}^{\mu\nu}_{xy}=\langle\psi^{\mu}_{\kappa}(\boldsymbol{k})|\partial_{k_x}|\psi^{\nu}_{\kappa}(\boldsymbol{k})\rangle\langle\psi^{\nu}_{\kappa}(\boldsymbol{k})|\partial_{k_y}|\psi^{\mu}_{\kappa}(\boldsymbol{k})\rangle. \tag{48}$$

The intrinsic Hall conductivity can be obtained through the relation

$$\sigma^{\rm II}_{\rm aH}=\sigma^{\rm c}_{\rm aH}+\sigma^{\rm v}_{\rm aH}=\lim_{q\to0}\frac{\Pi^{\rm II}_{0x}(q)}{|\boldsymbol{q}|}. \tag{49}$$

If the Fermi energy is tuned to the Weyl nodes ($E_{\rm F}=0$), for which only the valence band contributes to the Hall conductivity, we can obtain the intrinsic Hall conductivity in the dc limit as

$$\sigma^{\rm II}_{\rm aH}=\sigma^{\rm v}_{\rm aH}=\frac{e^2}{\hbar}\int\frac{{\rm d}^3\boldsymbol{k}}{(2\pi)^3}\sum_{\kappa}(\mathcal{B}^{\rm vc}_{xy}-\mathcal{B}^{\rm cv}_{xy}), \tag{50}$$

where we have used the fact that the occupation of states in valance bands is one (the Fermi function $n_{\rm F}(E^{\rm v}_{\kappa}(\boldsymbol{k}))=1$) and the occupation of states in conduction bands is zero ($n_{\rm F}(E^{\rm c}_{\kappa}(\boldsymbol{k}))=0$) at zero temperature. One can easily find that $F^{\rm v}_{\kappa}=\mathcal{B}^{\rm vc}_{xy}-\mathcal{B}^{\rm cv}_{xy}$. Obviously, Eqs. (50) and (16) are equivalent. In this case, one finds that only the $\kappa=-1$ sector survives in the integration in Eq. (50). Equation (50) is still well-defined when the Fermi level stays in the conduction band, where we just need to replace the Fermi distribution function for the conduction band by $\Theta(E_{\rm F}-E^{\rm c}_{\kappa}(\boldsymbol{k}))$. The Berry curvature for the conduction band can be obtained in the same way as Eq. (12), which has the form

$$F^{\rm c}_{\kappa}(\boldsymbol{k}_{\parallel},k_z)=\frac{1}{2k_{\parallel}}\frac{\partial}{\partial k_{\parallel}}P^{\rm c}_{\kappa}(k_{\parallel},k_z), \tag{51}$$

with

$$\begin{aligned}P^{\rm c}_{\kappa}(k_{\parallel},k_z) &= 2{\rm i}\langle\psi^{\rm c}_{\kappa}(\boldsymbol{k})|\partial_{\varphi_{\boldsymbol{k}_{\parallel}}}|\psi^{\rm c}_{\kappa}(\boldsymbol{k})\rangle\\ &=\frac{1}{2}(1+\cos2\alpha_{\boldsymbol{k}\kappa}).\end{aligned} \tag{52}$$

The Hall conductivity from the contribution of the conduction band may now be evaluated as

$$\sigma^{\rm c}_{\rm aH}=\frac{e^2}{\hbar}\int_{\rm BZ}\frac{{\rm d}k_z}{2\pi}\frac{1}{2}(1+\cos2\alpha_{\boldsymbol{k}\kappa})\Big|_0^{\sqrt{k_{\rm F}^2-k_z^2}}, \tag{53}$$

where $k_{\rm F}$ is the Fermi wave vector, which can be solved by the relation $E^{\rm c}_{\kappa}(\boldsymbol{k})=E_{\rm F}$. We repeat the discussion in the last subsection. For the case (i), the integral of k_z from zero to the Fermi energy in Eq. (53) becomes small due to the odd property of function $\cos2\alpha_{\boldsymbol{k}\kappa}$. The total anomalous Hall conductivity becomes

$$\sigma_{\rm aH}=\sigma^{\rm v}_{\rm aH}+\sigma^{\rm c}_{\rm aH}. \tag{54}$$

Therefore, the $\sigma_{\rm aH}$ deviates from the quantized value slowly as shown in Fig. 4(b), in which it can be found that if the Fermi energy is near the Weyl nodes, the Hall conductivity is not effected by the disorder significantly. While the Fermi energy is apart from the Weyl nodes, the behavior of the Hall conductivity is just like in normal metal phase.[47] For the case (ii), both of two sectors $\kappa=\pm1$ contribute to the intrinsic Hall conductivity, leading a fast deviation from the quantized value, as Fig. 4(b) shows.

4. Conclusion

We have analyzed the effects of an incident circular polarized light to a 3D topological insulator, we find that the topological phases and transport phenomena of the system can be tuned by varying the intensity of the light, under which the Weyl semimetal phase and anomalous Hall effect can emerge. Our proposal can be verified via the pump-probe angle-resolved photoemission spectroscopy (ARPES).[4,50,51] Our result provides a guidance for realizing Weyl materials and topological material engineering.

References

[1] Oka T and Aoki H 2009 *Phys. Rev. B* **79** 081406
[2] Lindner N H, Refael G and Galitski V 2011 *Nat. Phys.* **7** 490
[3] Rudner M S, Lindner N H, Berg E and Levin M 2013 *Phys. Rev. X* **3** 031005
[4] Wang Y H, Steinberg H, Jarillo-Herrero P and Gedik N 2013 *Science* **342** 453
[5] Jotzu G, Messer M, Desbuquois R, Lebrat M, Uehlinger T, Greif D and Esslinger T 2014 *Nature* **515** 237
[6] Rechtsman M C, Zeuner J M, Plotnik Y, Lumer Y, Podolsky D, Dreisow F, Nolte S, Segev M and Szameit A 2013 *Nature* **496** 196

[7] Tahir M, Manchon A and Schwingenschlögl U 2014 *Phys. Rev. B* **90** 125438
[8] Chen M N, Su W, Deng M X, Ruan J W, Luo W, Shao D X, Sheng L and Xing D Y 2016 *Phys. Rev. B* **94** 205429
[9] Hübener H, Sentef M A, Giovannini U D, Kemper A F and Rubio A 2017 *Nat. Commun.* **8** 13940
[10] Yan Z B and Wang Z 2016 *Phys. Rev. Lett.* **117** 087402
[11] Yan Z B and Wang Z 2017 *Phys. Rev. B* **96** 041206
[12] Chan C K, Oh Y T, Han J H and Lee P A 2016 *Phys. Rev. B* **94** 121106
[13] Narayan A 2016 *Phys. Rev. B* **94** 041409
[14] Taguchi K, Xu D H, Yamakage A and Law K T 2016 *Phys. Rev. B* **94** 155206
[15] Ezawa M 2017 *Phys. Rev. B* **95** 205201
[16] Yan Z B and Wang Z 2017 *Phys. Rev. B* **96** 041206
[17] Yao S Y, Yan Z B and Wang Z 2017 *Phys. Rev. B* **96** 195303
[18] Yan Z B, Bi R, Shen H T, Lu L, Zhang S C and Wang Z 2017 *Phys. Rev. B* **96** 041103
[19] Bomantara R W, Raghava G N, Zhou L and Gong J 2016 *Phys. Rev. E* **93** 022209
[20] Wang R, Wang B, Shen R, Sheng L and Xing D Y 2014 *Europhys. Lett.* **105** 17004
[21] Zhang X X, Ong T T and Nagaosa N 2016 *Phys. Rev. B* **94** 235137
[22] Zhou L, Chen C and Gong J 2016 *Phys. Rev. B* **94** 075443
[23] Wang H Q, Chen M N, Bomantara R W, Gong J and Xing D Y 2017 *Phys. Rev. B* **95** 075136
[24] Zhang D Q, Wang H Q, Ruan J W, Yao G and Zhang H J 2018 *Phy. Rev. B* **97** 195139
[25] Bomantara R W and Gong J 2018 *Phys. Rev. Lett* **120** 230405
[26] Chen M N, Mei F, Su W, Wang H Q, Zhu S L, Sheng L and Xing D Y 2017 *J. Phys. Condens. Matter* **29** 035601
[27] Cheng Q Q, Pan Y M, Wang H Q, Zhang C S, Yu D, Gover A, Zhang H J, Li T, Zhou L and Zhu S N 2019 *Phys. Rev. Lett.* **122** 173901
[28] Kitagawa T, Berg E, Rudner M and Demler E 2010 *Phys. Rev. B* **82** 235114
[29] Carpentier D, Delplace P, Fruchart M and Gawedzki K 2015 *Phys. Rev. Lett.* **114** 106806
[30] Yao N Y, Potter A C, Potirniche I D and Vishwanath A 2017 *Phys. Rev. Lett.* **118** 030401
[31] Wan X, Turner A M, Vishwanath A and Savrasov S Y 2011 *Phys. Rev. B* **83** 205101
[32] Parameswaran S A, Grover T, Abanin D A, Pesin D A and Vishwanath A 2014 *Phys. Rev. X* **4** 031035
[33] Burkov A A and Balents L 2011 *Phys. Rev. Lett.* **107** 127205
[34] Potter A C, Kimchi I and Vishwanath A 2014 *Nat. Commun.* **5** 5161
[35] Soluyanov A A, Gresch D, Wang Z, Wu Q, Troyer M, Dai X and Bernevig B A 2015 *Nature* **527** 495
[36] Wang Z, Gresch D, Soluyanov A A, Xie W, Kushwaha S, Dai X, Troyer M, Cava R J and Bernevig B A 2016 *Phys. Rev. Lett.* **117** 056805
[37] Xu S Y, Belopolski I, Alidoust N, Neupane M, Bian G, Zhang C, Sankar R, Chang G, Yuan Z, Lee C C, Huang S M, Zheng H, Ma J, Sanchez D S, Wang B, Bansil A, Chou F, Shibayev P P, Lin H, Jia S and Hasan M Z 2015 *Science* **349** 613
[38] Inoue H, Gyenis A, Wang Z, Li J, Oh S W, Jiang S, Ni N, Bernevig B A and Yazdani A 2016 *Science* **351** 1184
[39] Lv B Q, Weng H M, Fu B B, Wang X P, Miao H, Ma J, Richard P, Huang X C, Zhao L X, Chen G F, Fang Z, Dai X, Qian T and Ding H 2015 *Phys. Rev. X* **5** 031013
[40] Deng K, Wan G, Deng P, Zhang K, Ding S, Wang E, Yan M, Huang H, Zhang H, Xu Z, Denlinger J, Fedorov A, Yang H, Duan W, Yao H, Wu Y, Fan S, Zhang H, Chen X and Zhou S 2016 *Nat. Phys.* **12** 1105
[41] Huang L, McCormick T M, Ochi M, Zhao Z, Suzuki M T, Arita R, Wu Y, Mou D, Cao H, Yan J, Trivedi N and Kaminski A 2016 *Nat. Mat.* **15** 115
[42] Kitagawa T, Oka T, Brataas A, Fu L and Demler E 2011 *Phys. Rev. B* **84** 235108
[43] Nandkishore R and Huse D A 2015 *Annu. Rev. Condens. Matter Phys.* **6** 15
[44] Zhang J, Hess P W, Kyprianidis A, Becker P, Lee A, Smith J, Pagano G, Potirniche I D, Potter A C, Vishwanath A, Yao N Y and Monroe C 2017 *Nature* **543** 217
[45] Zhang H J, Liu C X, Qi X L, Dai X, Fang Z and Zhang S C 2009 *Nat. Phys.* **5** 438
[46] Thouless D J, Kohmoto M, Nightingale M P and den Nijs M 1982 *Phys. Rev. Lett.* **49** 405
[47] Burkov A A 2014 *Phys. Rev. Lett.* **113** 187202
[48] Rammer J 2004 *Quantum Transport Theory* (Westview Press, Boulder, CO)
[49] Qi X L, Hughes T L and Zhang S C 2008 *Phys. Rev. B* **78** 195424
[50] Mahmood F, Chan C K, Alpichshev Z, Gardner D, Lee Y, Lee P A and Gedik N 2016 *Nat. Phys.* **12** 306
[51] Giovannini U D, Hübener H and Rubio A 2016 *Nano Lett.* **16** 7993